Supplementary Information for

Enhanced Stability and Linearly Polarized Emission from $CsPbI_3$ Perovskite Nanoplatelets through A-site Cation Engineering

Woo Hyeon Jeong[1,2], Junzhi Ye[2]*, Jongbeom Kim[3], Rui Xu[4], Xinyu Shen[1,5], Chia-Yu Chang[2], Eilidh L. Quinn[2], Hyungju Ahn[6], Myoung Hoon Song[3], Peter Nellist[7], Henry J. Snaith[5], Yunwei Zhang[4], Bo Ram Lee[1]* and Robert L. Z. Hoye[2]*

[1] School of Advanced Materials Science and Engineering, Sungkyunkwan University, Suwon, 16419, Republic of Korea

[2] Inorganic Chemistry Laboratory, University of Oxford, Oxford, OX1 3QR, United Kingdom

[3] Department of Materials Science and Engineering, Ulsan National Institute of Science and Technology (UNIST), Ulsan, 44919 Republic of Korea

[4] School of Physics, Sun Yat-sen University, Guangzhou, 510275 China

[5] Clarendon Laboratory, Department of Physics, University of Oxford, Oxford, OX1 3PU United Kingdom

[6] Pohang Accelerator Laboratory (PAL) Pohang, Gyeongbuk 37673, Republic of Korea

[7] Department of Materials, University of Oxford, Oxford OX1 3PH United Kingdom

*Correspondence: junzhi.ye@chem.ox.ac.uk (J.Y.), brlee@skku.edu (B.R.L.), robert.hoye@chem.ox.ac.uk (R.L.Z.H.)

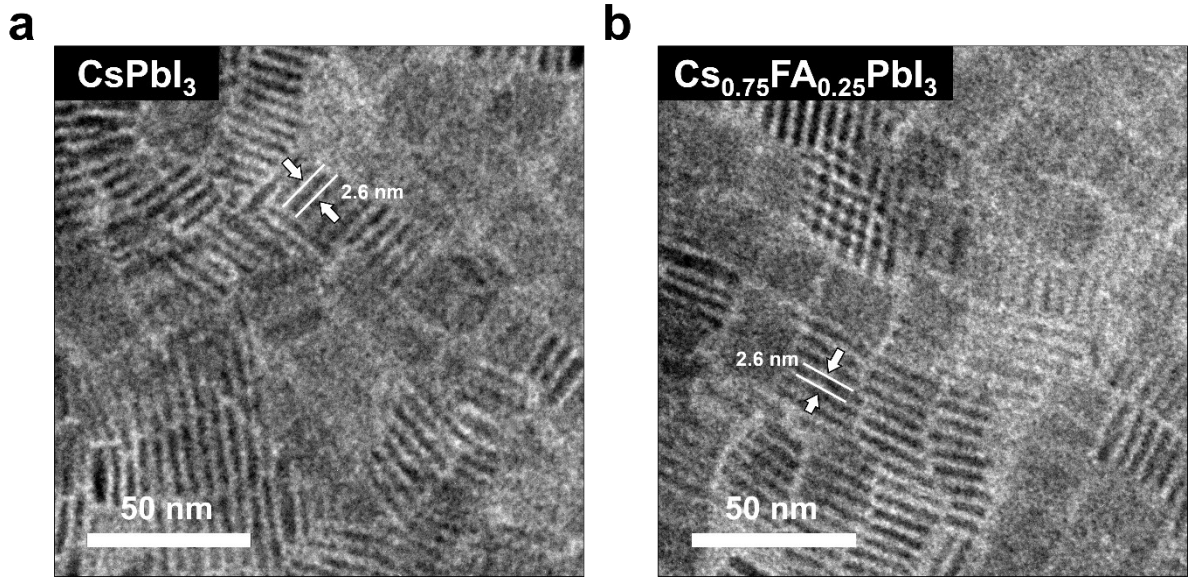

Figure S1. Transmission electron microscopy (TEM) image of **a** $CsPbI_3$ and **b** $Cs_{0.75}FA_{0.25}PbI_3$ PeNPLs. These nanoplatelets were dispersed in a hexane solvent, and drop cast onto a Cu TEM grid.

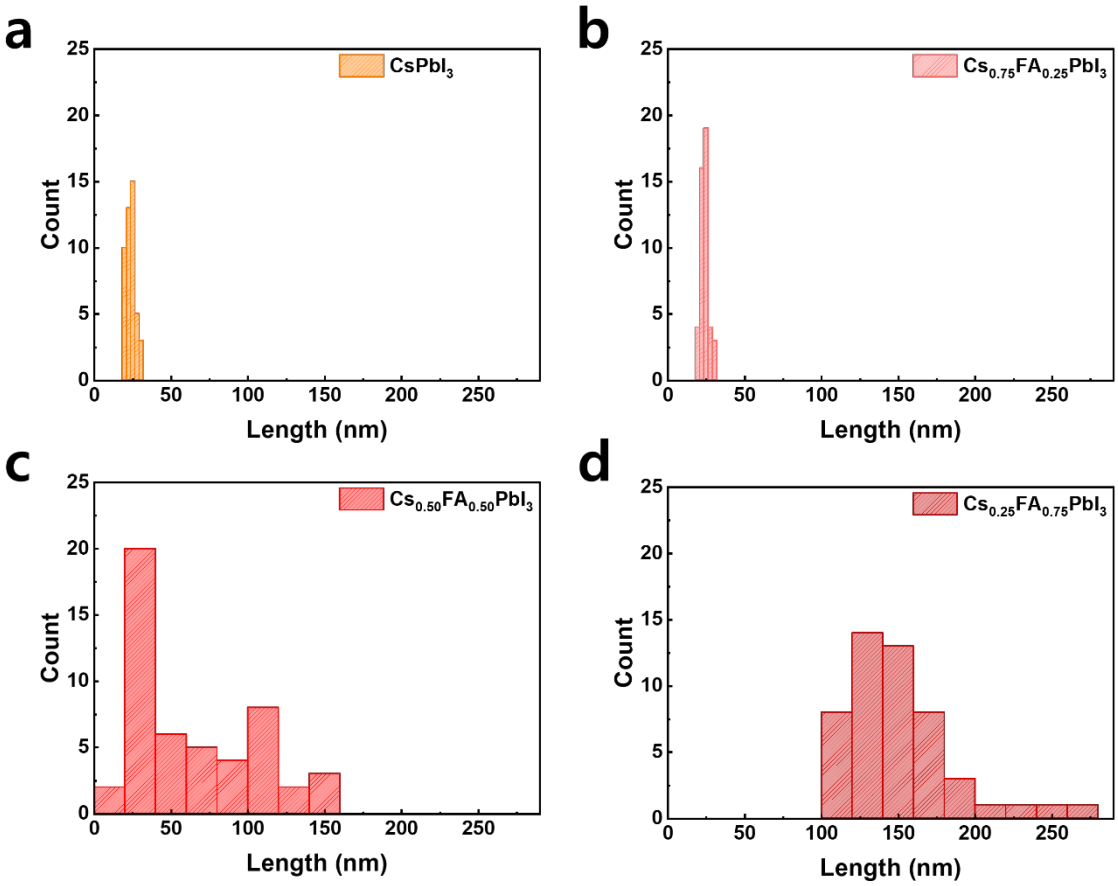

Figure S2. Size distribution histogram of **a** $CsPbI_3$, **b** $Cs_{0.75}FA_{0.25}PbI_3$, **c** $Cs_{0.50}FA_{0.50}PbI_3$ and **d** $Cs_{0.25}FA_{0.75}PbI_3$, determined from TEM measurements from Fig. 1a in the main text.

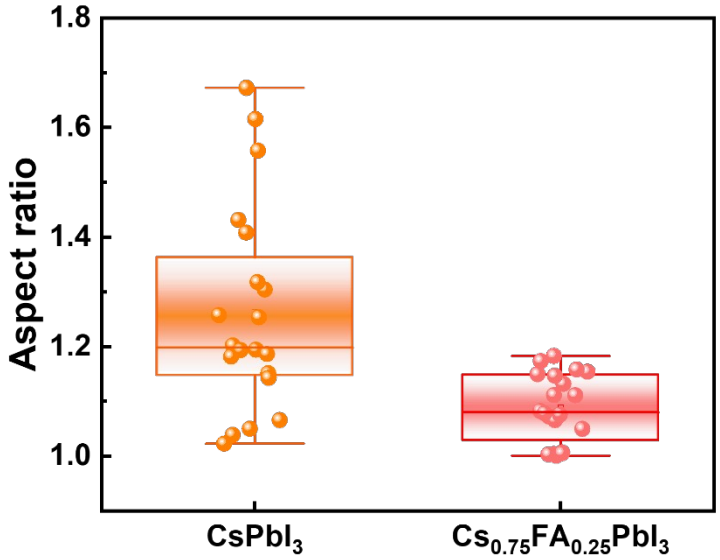

Figure S3. Distribution in the aspect ratio of PeNPLs. Data was collected from 20 individually-identified PeNPLs from Figure S1.

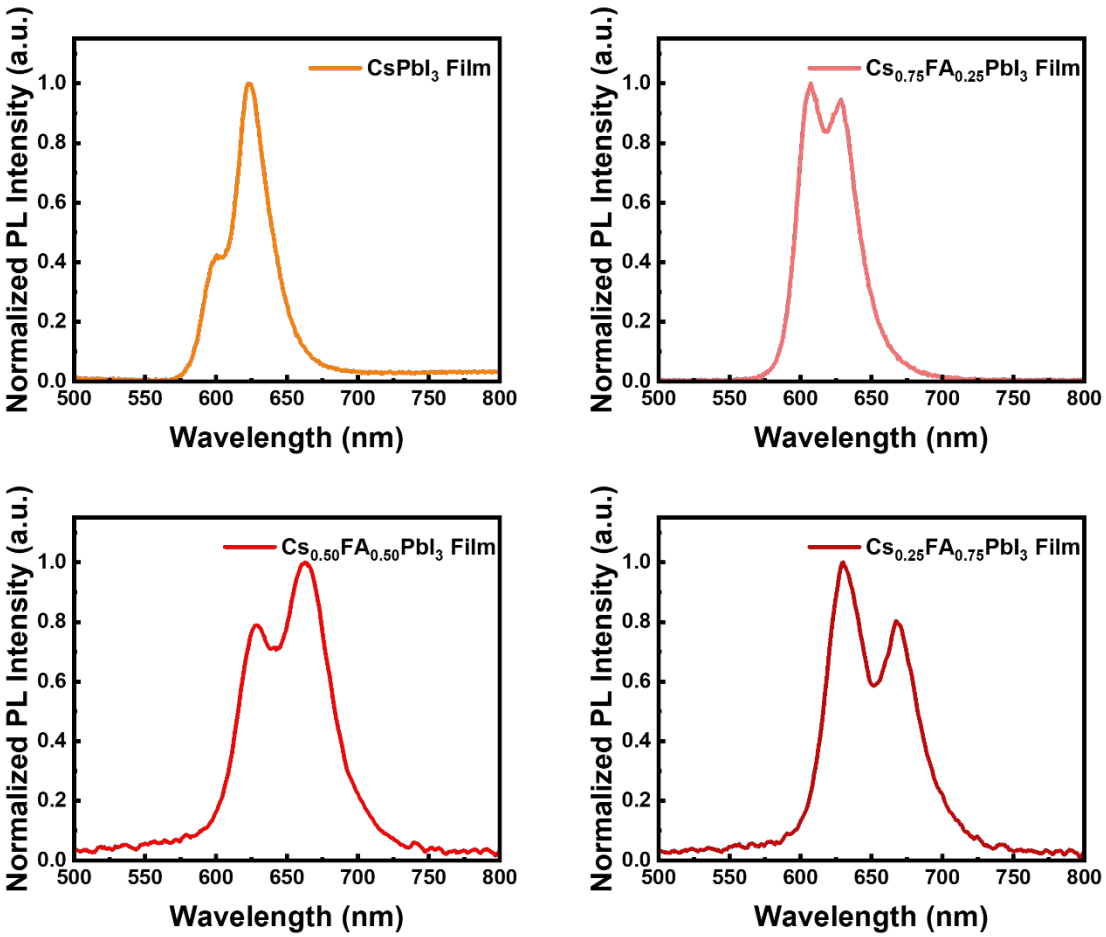

Figure S4. Photoluminescence spectra of (Cs,FA)PbI_3 PeNPLs drop-cast onto glass substrates. Samples were measured in an N_2-filled glovebox, excited with a 405 nm wavelength CW laser at 37.3 mW cm^{-2} power density.

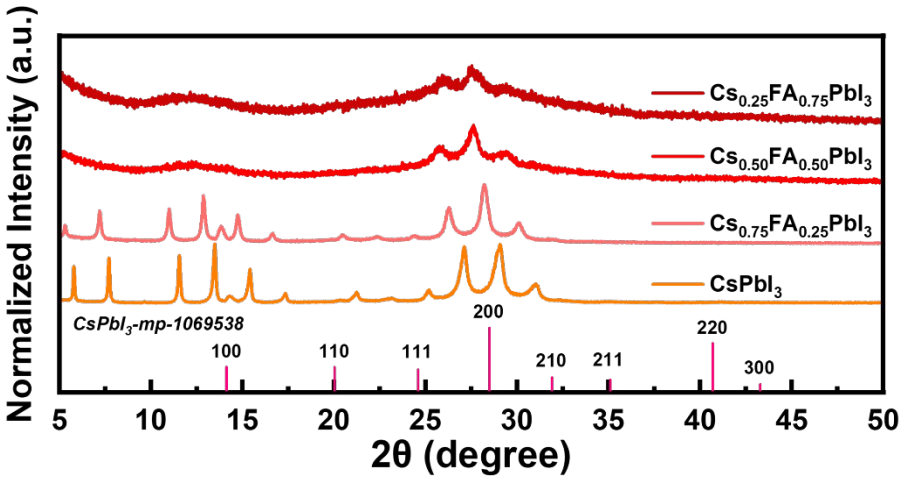

Figure S5. X-ray diffraction patterns of PeNPLs compared with the reference pattern for α-$CsPbI_3$ (mp-1069538)[1].

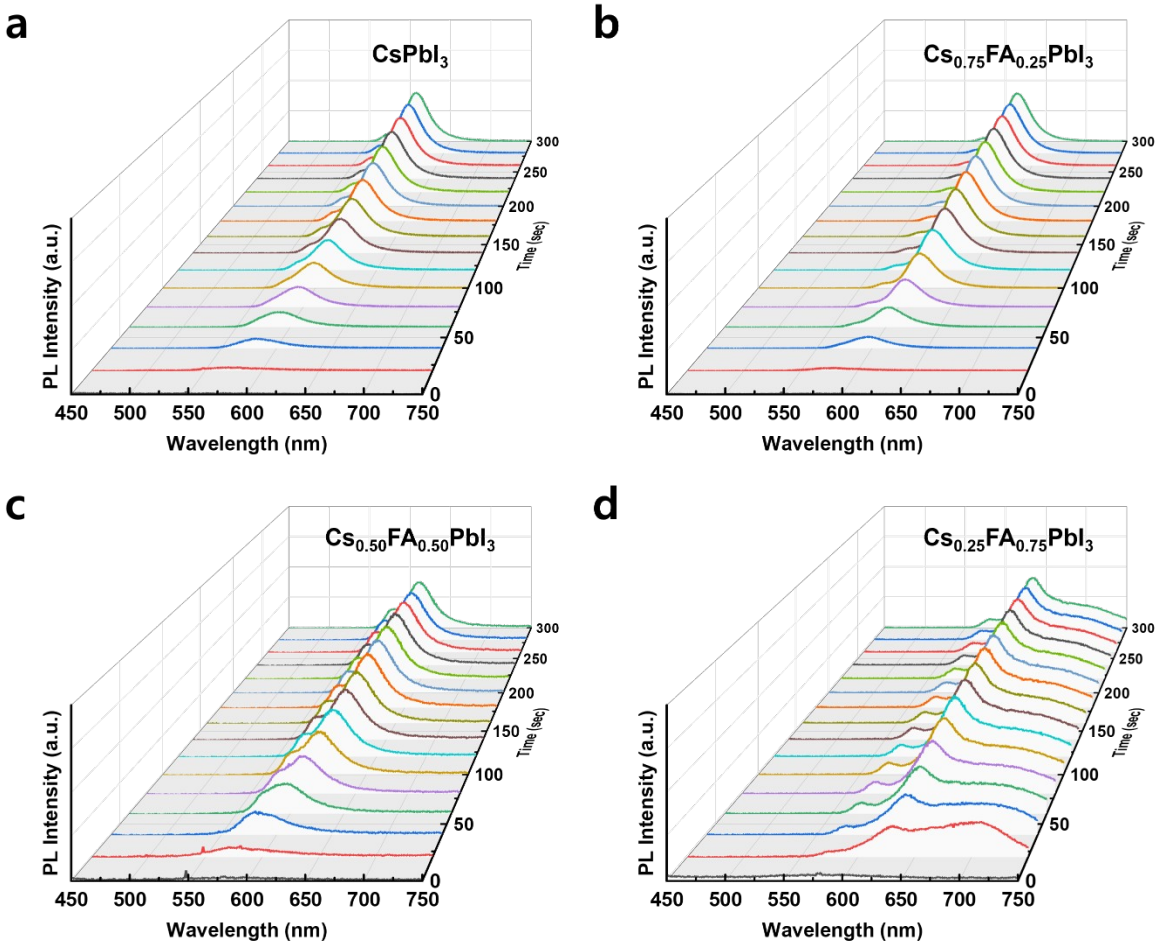

Figure S6. *In-situ* PL spectra during the formation of each PeNPL following the injection of the Cs-oleate/FA-oleate into the PbI_2-ligand solution. These spectra are displayed in Fig. 2b in the main text. Spectra obtained at 20 s time intervals. Samples were measured in an in ambient air during synthesis (see Methods in the main text), excited with a 405 nm wavelength CW laser at 37.3 mW cm^{-2} power density.

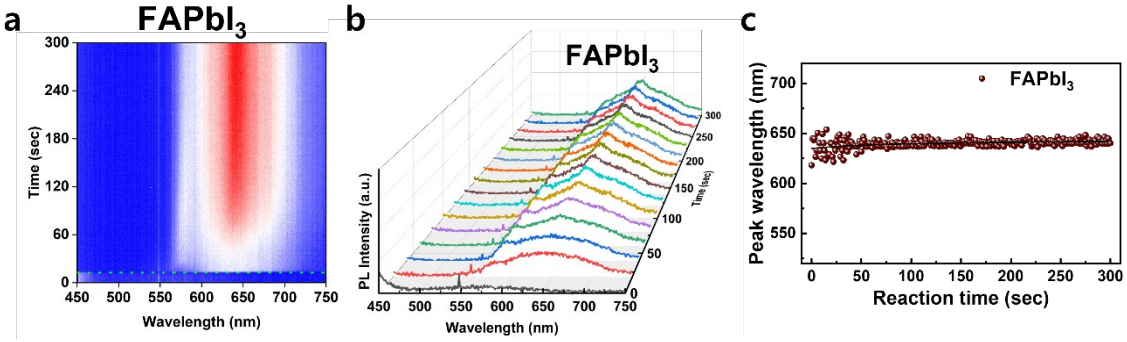

Figure S7. a, **b** *In-situ* PL spectra during the formation of $FAPbI_3$ PeNPLs. Spectra were collected at 20 s intervals from the time the FA-oleate was injected into the PbI_2-ligand solution. **c** Detailed kinetics of the photoluminescence peak wavelength evolution over time after injecting the FA oleate solution into the reaction mixture. Data points were collected at 1 s time intervals. Samples were measured in an in ambient air during synthesis (see Methods in the main text), excited with a 405 nm wavelength CW laser at 37.3 mW cm^{-2} power density.

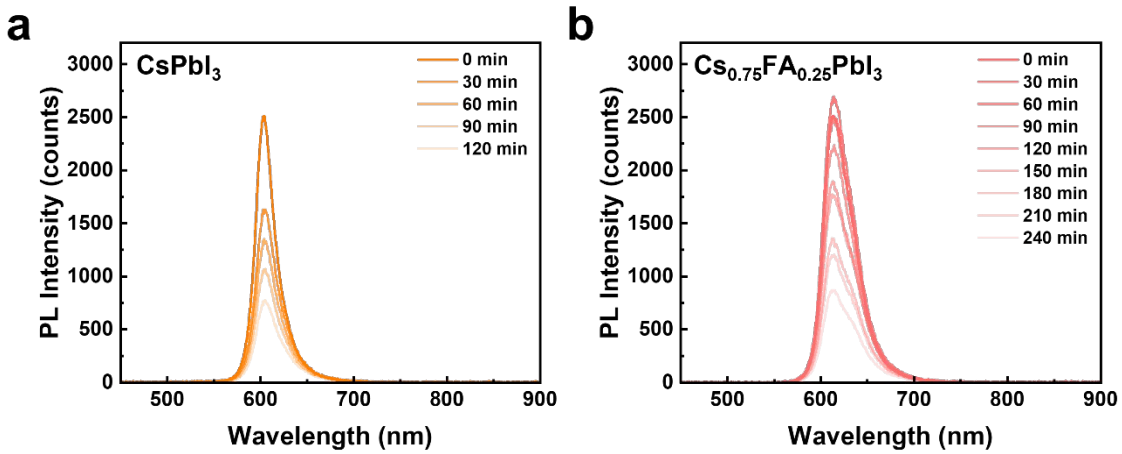

Figure S8. PL spectra of colloidal PeNPL solutions of **a** $CsPbI_3$ and **b** $Cs_{0.75}FA_{0.25}PbI_3$ heated to 80 °C as a function of time 0 to 240 min. Samples were measured at 80 ℃ in ambient air, excited with a 405 nm wavelength CW laser at 37.3 mW cm^{-2} power density.

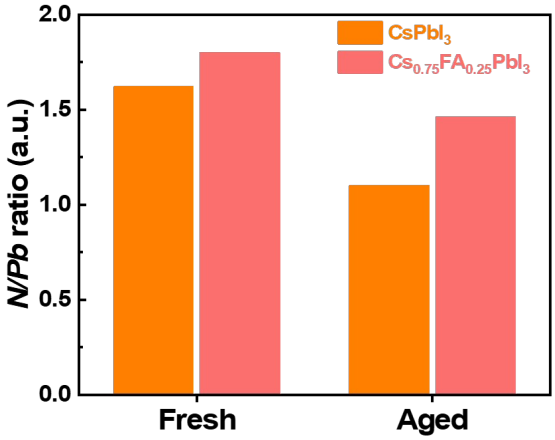

Figure S9. N/Pb ratios from XPS measurements of in $CsPbI_3$ and $Cs_{0.75}FA_{0.25}PbI_3$ PeNPLs before and after 7 days of ambient aging.

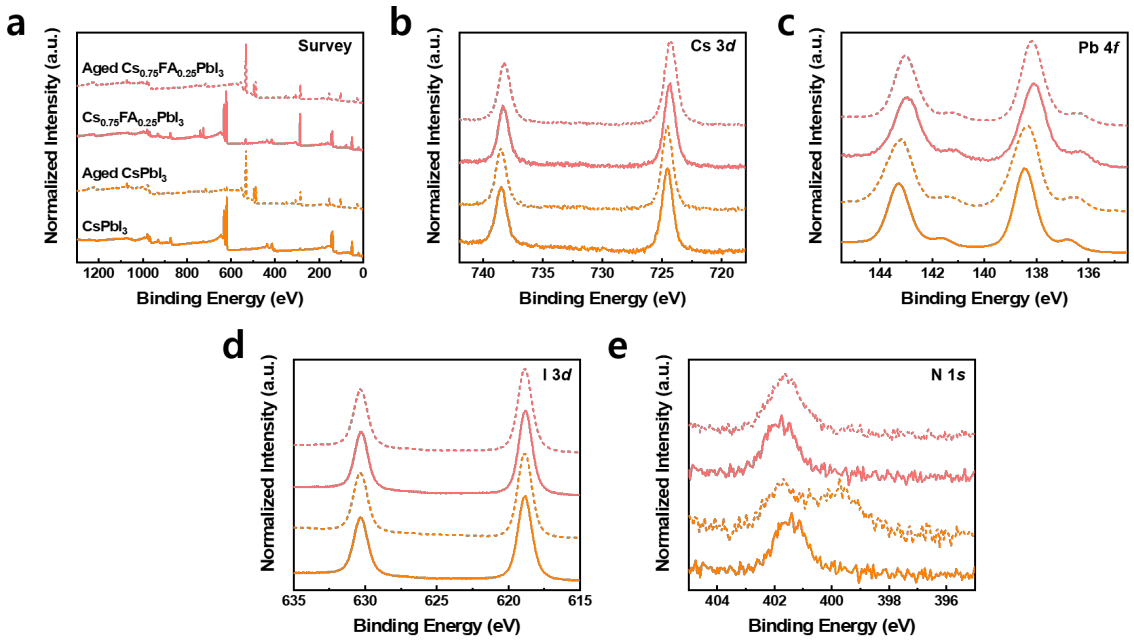

Figure S10. **a** Survey XPS spectra, **b** Cs 3d, **c** Pb 4f, **d** I 3d and **e** N 1s core level spectra of $CsPbI_3$ and $Cs_{0.75}FA_{0.25}PbI_3$ PeNPLs before and after 7 days of ambient aging.

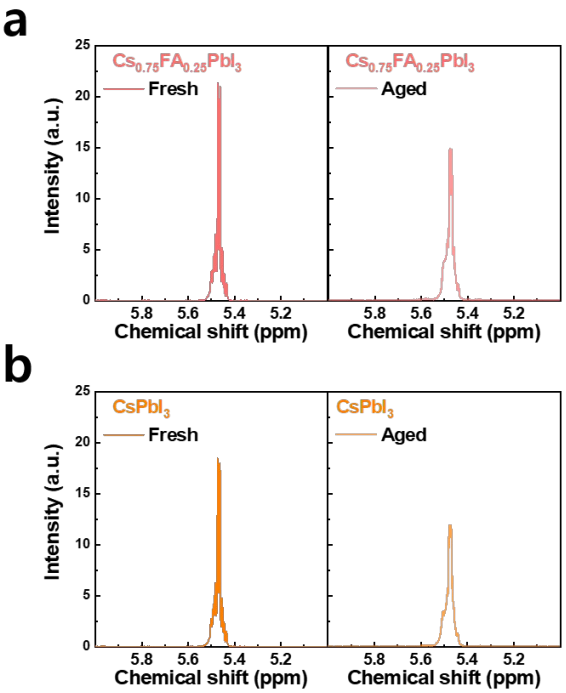

Figure S11. ^{1}H-NMR spectra of **a** $CsPbI_3$ and **b** $Cs_{0.75}FA_{0.25}PbI_3$ PeNPLs before and after 7 days of ambient aging.

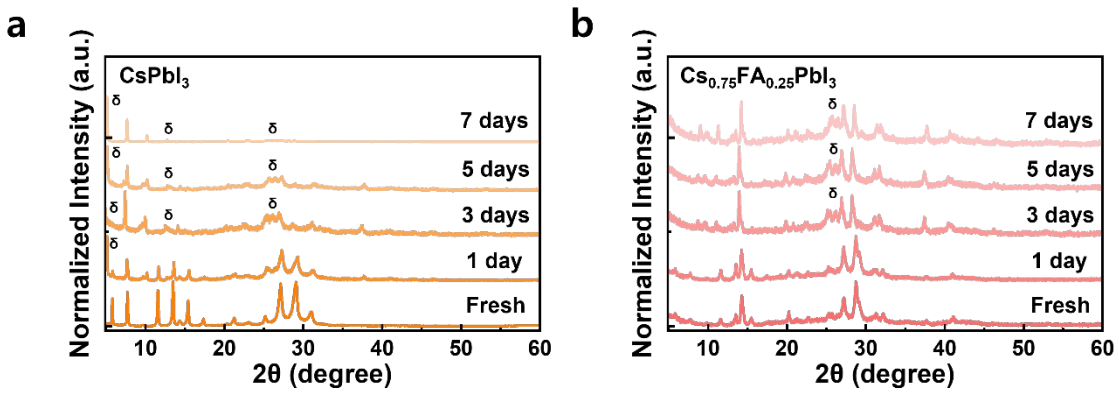

Figure S12. Change in the X-ray diffraction patterns of **a** $CsPbI_3$ and **b** $Cs_{0.75}FA_{0.25}PbI_3$ PeNPL films over time after storage in ambient conditions (40% relative humidity, 20 °C, stored in the dark).

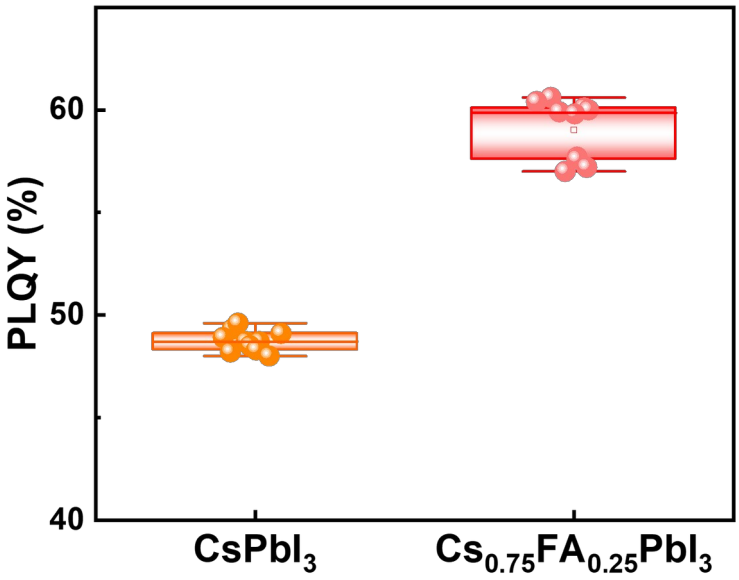

Figure S13. PLQY distributions of colloidal PeNPLs Samples were measured by Quantaurus-QY Absolute PL quantum yield spectrometer (HAMAMATSU).

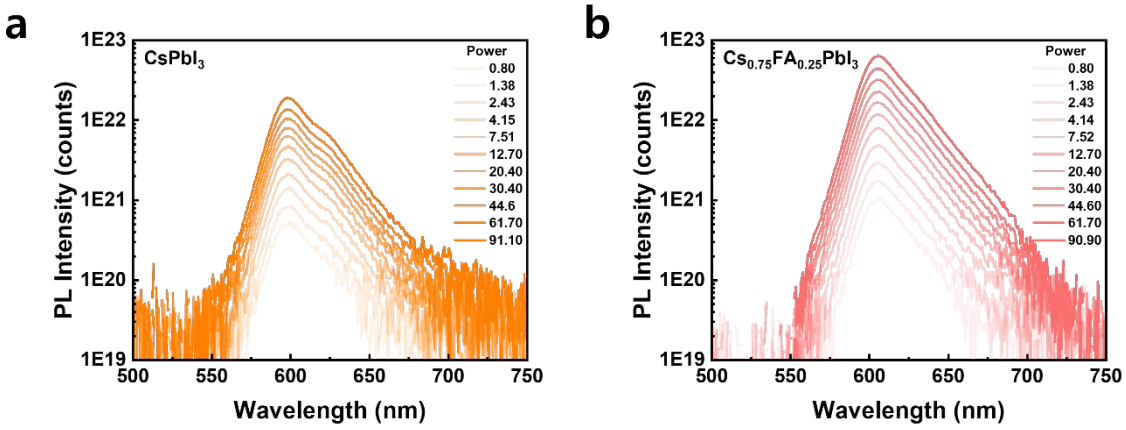

Figure S14. Change in the PL spectra of colloidal PeNPLs of **a** $CsPbI_3$ and **b** $Cs_{0.75}FA_{0.25}PbI_3$ depending on excitation power densities (in mW cm^{-2}) from Fig. 4a in the main text. Samples were measured in ambient air, and excited with a 405 nm wavelength CW laser.

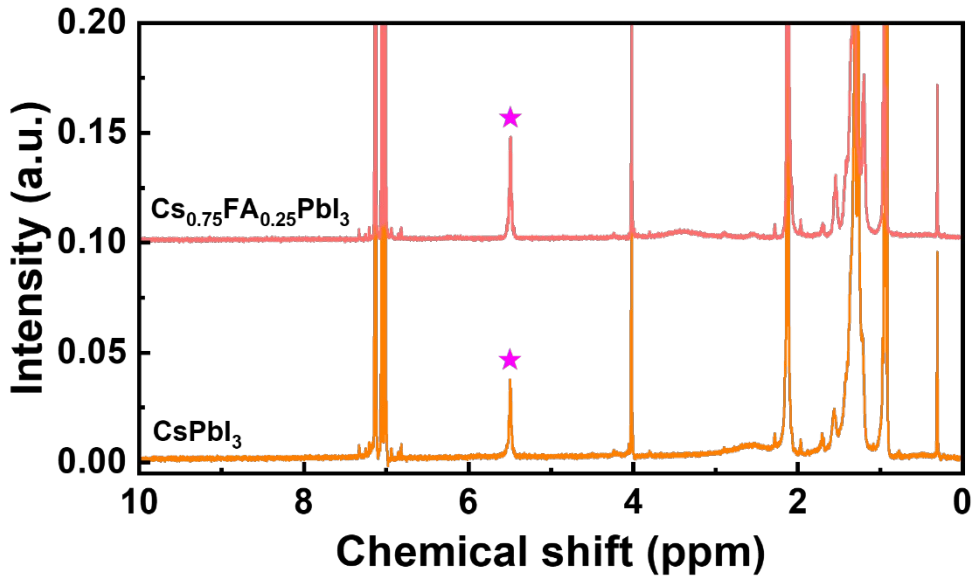

Figure S15. ^{1}H-NMR spectra of colloidal PeNPL solutions in deuterated-toluene. Magenta stars indicate peaks corresponding to the oleic acid and oleylamine ligands.

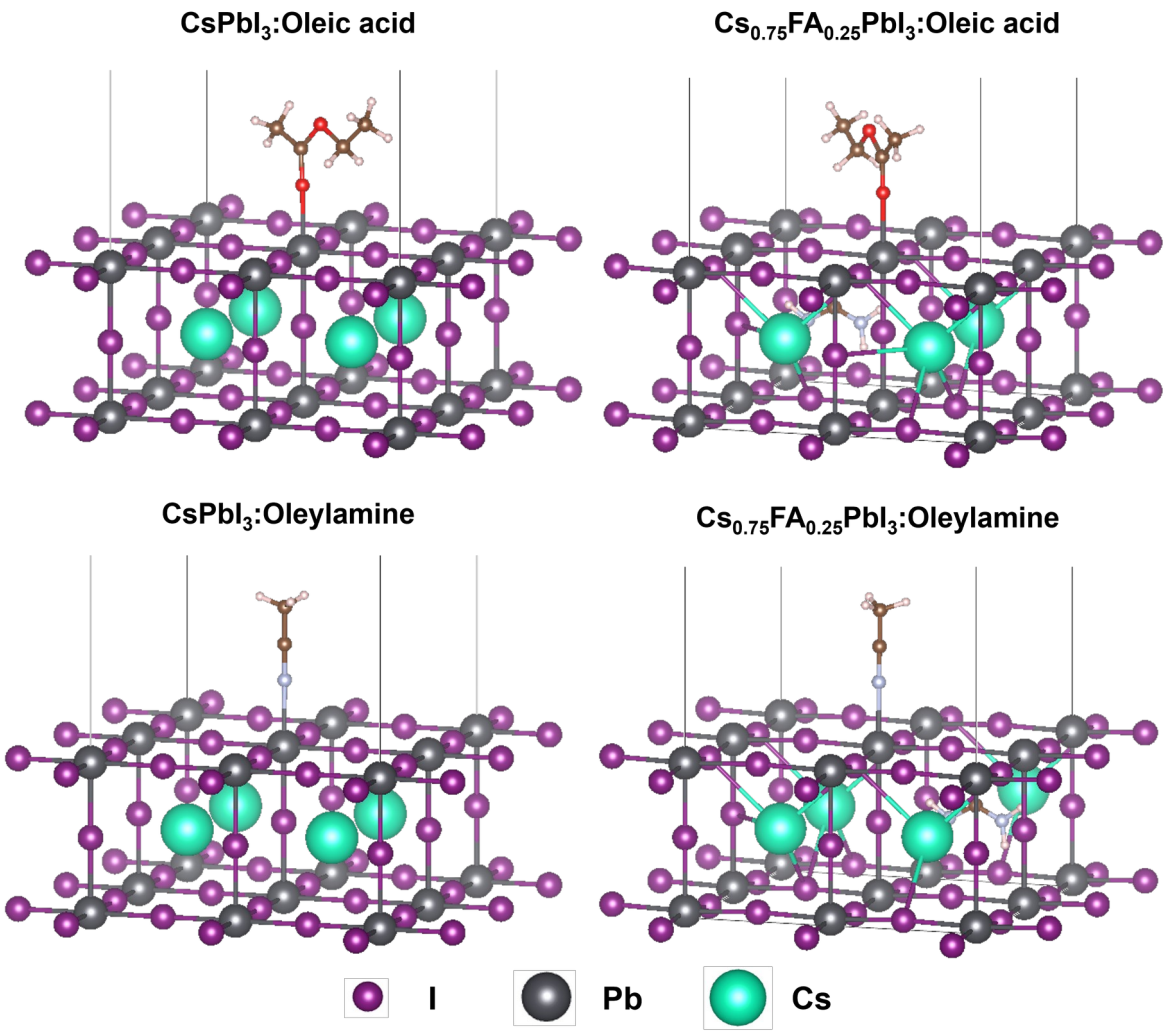

Figure S16. Calculation of the surface binding energy between the halide perovskite ($CsPbI_3$ and $Cs_{0.75}FA_{0.25}PbI_3$) and oleic acid and oleylamine ligand using electron localization functions from DFT.

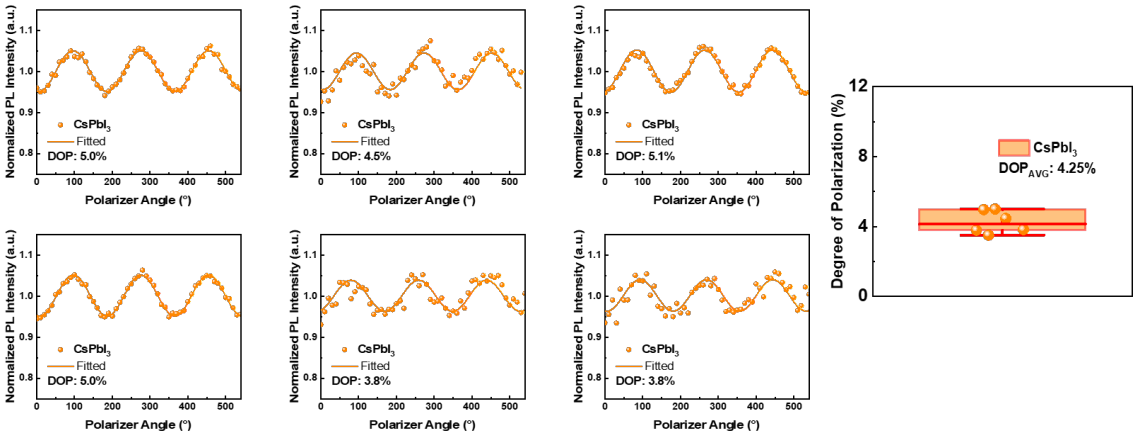

Figure S17. Polarization dependence of the normalized PL intensity of $CsPbI_3$ PeNPLs films made in different batches, along with the distribution in the degree of linear polarization (DOP) determined from these measurements. Measurements performed inside a N_2-filled glovebox with a 405 nm wavelength CW laser at 37.3 mW cm^{-2} power density.

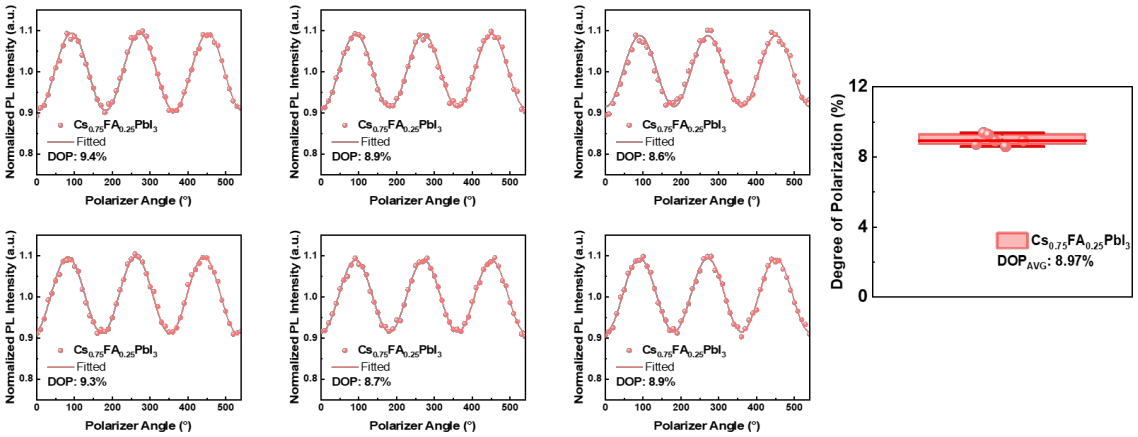

Figure S18. Polarization dependence of the normalized PL intensity of $Cs_{0.75}FA_{0.25}PbI_3$ PeNPLs film made in different batches, along with the distribution in the degree of linear polarization (DOP) determined from these measurements. Measurements performed inside a N_2-filled glovebox with a 405 nm wavelength CW laser at 37.3 mW cm^{-2} power density.

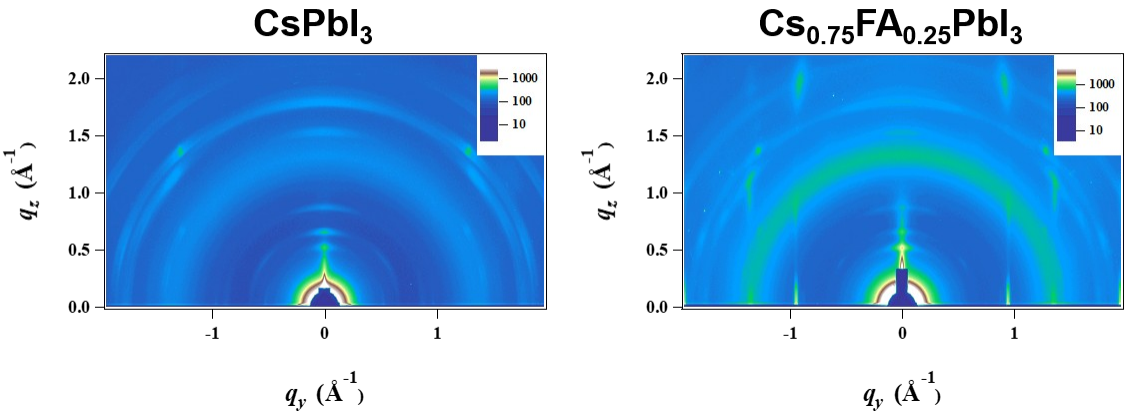

Figure S19. Grazing-incidence wide-angle X-ray scattering (GIWAXS) patterns of edge-up oriented $CsPbI_3$ and $Cs_{0.75}FA_{0.25}PbI_3$ PeNPL thin films. Sharper Bragg spots along q_z in the x = 0.25 PeNPL indicate improved vertical alignment of the PeNPL superlattice.

Table S1. XPS analysis of each PeNPLs.

Sample configuration	Atomic %			
	Cs	Pb	I	N
$CsPbI_3$	0.89	1.00	4.02	1.62
Aged-$CsPbI_3$	0.45	1.00	2.35	1.10
$Cs_{0.75}FA_{0.25}PbI_3$	0.76	1.00	4.01	1.80
Aged-$Cs_{0.75}FA_{0.25}PbI_3$	0.61	1.00	3.12	1.46

REFERENCES

1 Lin, C.-C. *et al.* Exploring the Origin of Phase-Transformation Kinetics of CsPbI3 Perovskite Nanocrystals Based on Activation Energy Measurements. *The Journal of Physical Chemistry Letters* **11**, 3287-3293 (2020). https://doi.org/10.1021/acs.jpclett.0c00443